Condition Evolution in Bridge Management Systems and Corrosion-Induced Deterioration

Guido Roelfstra[1]; Rade Hajdin[2]; Bryan Adey[3]; and Eugen Brühwiler[4]

Abstract: Condition assessment in the Swiss bridge management system (KUBA-MS) is performed on the element level. Five condition states are defined based on visual appearance. In order to forecast the condition states of any given element at any given time a relationship must be established between the element age and its condition state. This relationship, which describes the condition evolution, can be obtained empirically from statistical analysis of pairs of consecutive condition assessments (inspections). Markov chains are used in KUBA-MS to represent condition evolution and the transition probabilities are determined using regression analysis of pairs of inspections. Unfortunately there are almost no inspection data for the worst and second worst condition states. The forecasts made using Markov chains are therefore not always reliable. In this paper an alternative approach is suggested, which takes into consideration the physical phenomena underlying element deterioration. This alternative approach is applied to chloride-induced corrosion of steel reinforcement, by far the most common deterioration mechanism in Switzerland. The chloride-induced corrosion is modeled mathematically and numerical simulations of the condition evolution for different values of model parameters are performed. The simulation results have been mapped to condition states as defined in KUBA-MS and Markov transition matrices have been calibrated to fit simulation results.

Introduction

The construction of the Swiss National Highway System began in the 1960s. Currently over 87% has been completed. Due to Switzerland's mountainous topography, road structures are a crucial part of this system. In total 3,400 bridges have been built with a total length of 267 km. The vast majority (over 95%) of bridges are constructed in reinforced or prestressed concrete and the remaining bridges (less than 5%) are composite structures.

With the imminent completion of the national highway system, the main effort of public authorities has shifted from the construction of new structures toward the preservation of existing ones. As part of this effort, the Swiss federal road authorities developed a bridge management system (BMS) called KUBA-MS (*KUBA-MS-Ticino* 1998). Similar to other bridge management systems KUBA-MS suggests preservation actions based on the condition

of bridge elements and computes the financial needs to perform these actions. A crucial component in KUBA-MS is the deterioration model, which allows the element condition to be predicted for any given point in time in the future. Currently, the assessment and forecast of the condition of bridge elements (e.g., deck, joints, piers, etc.), is based on visual inspection and comparison of the observed damage with commonly recognized damage patterns for each condition state.

The condition evolution of an element is described by a function of a discrete variable. The possible values of the discrete variable represent condition states (Table 1). Since the condition evolution cannot be predicted deterministically the discrete variable is randomized. This yields the probabilities of an element being in each of the condition states as a function of time. This function is determined empirically in all currently available BMS. In most cases Markov chains are used for this purpose and corresponding transition probabilities are obtained statistically using both inspection results of a large sample of bridges and expert opinions.

It is, however, possible and desirable to develop a theoretical deterioration model based on the physical and chemical processes that cause the deterioration. Due to recent advances, the deterioration phenomena are well understood and for a number of them, e.g., chloride-induced corrosion, analytical models that can adequately mimic reality have been developed. Unfortunately these models cannot be directly integrated into BMSs since they require data that cannot be collected economically by the available onsite inspection techniques.

In this paper a theoretical model is used to simulate the deterioration of reinforced concrete due to chloride-induced corrosion. Due to the types of bridges in the Swiss Highway System this is the predominant damage mechanism in Switzerland. The model uses quantitative parameters related to concrete properties that can be measured by available inspection techniques. For given environmental actions, i.e., temperature, humidity, and salt

[1]Dr. of Civil Engineering, Bonnard et Gardel S.A., Ave. de Cour 61, CP 241, CH 1001 Lausanne, Switzerland.

[2]Visiting Professor Dr. of Systems Engineering, Dept. of Electrical and Systems Engineering, Univ. of Pennsylvania, 220 South 33rd St., 270 Towne Building, Philadelphia, PA 19104-6315.

[3]Dr. of Civil Engineering, Swiss Federal Institute of Technology, School of Architecture, Civil and Environmental Engineering, Maintenance and Safety of Structures Division (MCS), CH 1015 Lausanne, Switzerland.

[4]Professor Dr. of Civil Engineering, Swiss Federal Institute of Technology, School of Architecture, Civil and Environmental Engineering, Maintenance and Safety of Structures Division (MCS), CH 1015 Lausanne, Switzerland.

Table 1. Condition States Defined in Swiss Bridge Management System (*KUBA-MS-Ticino* 1998)

Condition state		Description
1	Good	No visible damage; only thin superficial cracks; no signs of corrosion
2	Acceptable	Visible spots of rust and/or local spalling; thin cracks due to corrosion of the reinforcement and/or humid zones; insignificant mechanical damage
3	Damaged	Spalling with visible reinforcement, insignificant loss of section, less than 10% than visible reinforcement; cracks and/or humid zones
4	Bad condition	Spalling with visible reinforcement, significant loss of section, more than 10% of reinforcement visible; cracks and/or humid zones
5	Alarming	The structure is in danger, measures are necessary before next principal inspection; immediate measures

concentration, the extent of deterioration (e.g., section loss of reinforcement bars) can be obtained in a quantitative manner. These quantitative values can be mapped to the condition states currently used in BMSs and used to determine the Markov transition probabilities.

Assessment and Forecast of Condition in Bridge Management Systems

Condition States

Currently, during visual inspection condition states are attributed to elements according to the observed damage. In most BMSs the condition states are verbally described (Table 1) and illustrated by photos showing commonly recognized damage.

Since the condition states have been established based on visual appearance, they are not directly related to the structural behavior of the bridge (structural safety and serviceability). Structural safety is only directly mentioned in condition State 5, where a safety problem is suspected and an urgent intervention is anticipated. This widespread practice should be questioned as for some elements even the complete loss of structural resistance may not be significant for overall structural performance and for other elements even small losses may be very significant. It is, however, generally assumed that these preservation actions will be performed before any significant impairment of the overall bridge performance. In other words the preservation policy must not allow elements to enter the worst condition state. The condition assessment in BMSs will therefore give little insight into the functional or structural performance of a bridge. Its purpose is to serve as a basis for planning of preservation actions. The definition of condition states is therefore chosen in such a manner that feasible preservation actions and their unit costs can be easily identified for each condition state and catalogued within BMSs.

Segmental Inspection

The assessment unit in most BMSs is a structural element, e.g., deck, joints, and piers. This presumes that the entire element exhibits the same characteristics and is exposed to the same environmental and mechanical actions. This is in some cases highly improbable, especially for large elements. It is therefore often

necessary to divide elements into segments. In KUBA-MS, the elements are divided into segments that exhibit homogeneous concrete properties and experience similar actions. A uniform condition evolution within a segment can therefore be expected.

Condition Evolution

The condition of a segment (CS) is described by a probability mass function represented by five scalars and thus often called a condition state vector. Each scalar can be interpreted either as:
1. The probability of a segment to be in one of the five condition states or
2. The percentage of a segment in each condition state (the condition state vector resulting from inspections, which represents current condition, have normally only one nonzero scalar).

Since the condition evolution in KUBA-MS is modeled using Markov chains the condition state vector of a bridge segment at time $t+1$ is obtained by multiplying the condition state vector of the segment at time t by the deterioration matrix a_{ij} [Eq. (1)]. The interval between time $t+1$ and time t is given by the inspection period

$$
\begin{matrix} CS1: \\ CS2: \\ CS3: \\ CS4: \\ CS5: \end{matrix}
\begin{pmatrix} x_1 \\ x_2 \\ x_3 \\ x_4 \\ x_5 \end{pmatrix}_{t+1}
=
\begin{bmatrix} a_{11} & a_{12} & a_{13} & a_{14} & a_{15} \\ 0 & a_{22} & a_{23} & a_{24} & a_{25} \\ 0 & 0 & a_{33} & a_{34} & a_{35} \\ 0 & 0 & 0 & a_{44} & a_{45} \\ 0 & 0 & 0 & 0 & a_{55} \end{bmatrix}^T
\times
\begin{pmatrix} x_1 \\ x_2 \\ x_3 \\ x_4 \\ x_5 \end{pmatrix}_{t}
$$

(1)

The coefficients of matrix a_{ij} can be interpreted in two ways as follows:
1. As the percentage of a segment that changed from condition state i to condition state j after one inspection period, or
2. As the probability of a unit quantity of a segment to pass from condition state i to condition state j after one inspection period.

The deterioration matrices in a BMS are often determined by statistical analysis. However in the case of a lack of data they can be determined based on expert opinions. Expert opinions were used in KUBA-MS to obtain transition probabilities between condition States 3, 4, and 5.

The concrete properties and exposure to environmental and mechanical actions are only implicitly considered in KUBA-MS, by introducing three different deterioration rates: slow, medium, and fast. For example, in the case of aggressive environmental actions and poor concrete properties, which were observed during inspections, the fast deterioration rate would be expected.

Based on collected data the deterioration rates are defined as follows:
- Slow: 50% probability of a segment being in condition State 1 or 2 after 120 years;
- Medium: 50% probability of a segment being in condition State 1 or 2 after 80 years; and
- Fast:: 50% probability of a segment being in condition State 1 or 2 after 40 years.

Chloride-Induced Corrosion

Phenomenon

During cement hydration, a highly alkaline pore solution (pH 12.5–13.6) is formed in the concrete. In this alkaline environ-

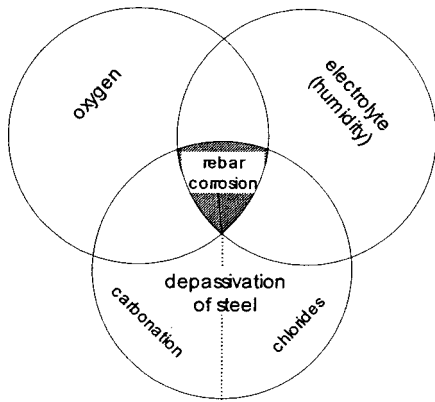JOURNAL OF BRIDGE ENGINEERING © ASCE / MAY/JUNE 2004 / **269**

Fig. 1. Prerequisites for steel reinforcement corrosion in concrete

ment, ordinary reinforcing steel forms a very thin oxide film (the passive film) that protects the steel from corrosion. This passive film remains stable as long as the composition of the pore solution remains constant. The protective film is destroyed when there is a sufficient concentration of chloride ions around the reinforcement. The chloride ions, stemming from deicing salts, penetrate into concrete from the road surface. Once the reinforcing steel is depassivated and it is supplied with oxygen and water (humidity), metal dissolution (corrosion in the form of rust formation, loss in cross section) may start (Fig. 1).

The deterioration of concrete element due to reinforcement corrosion can be divided into two phases (Fig. 2) as follows:

1. During the initiation phase, chlorides penetrate from the surface of the concrete to the reinforcement. The initiation phase starts with the construction of the structure and ends with the depassivation of the reinforcing steel.
2. During the propagation phase, the reinforcement actively corrodes. The duration of the propagation phase depends on the corrosion rate. The propagation phase begins with the depassivation of the reinforcing steel and ends with the structural failure or complete dissolution of reinforcement steel.

A durable concrete structure should have both a long initiation phase and a long propagation phase, i.e., slow corrosion rate.

It is well established that the chloride penetration and depassivation of the reinforcement are governed by the concrete cover thickness, the concrete porosity, i.e., permeability of concrete cover, the concentration of chlorides, and the microclimatic conditions (wetting, drying, and temperature) of the concrete. The propagation phase, i.e., corrosion rate, is governed by the electri-
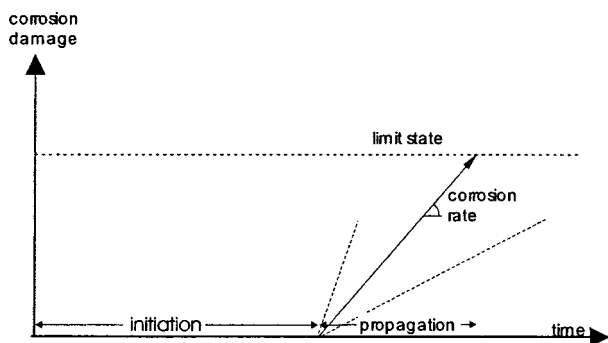

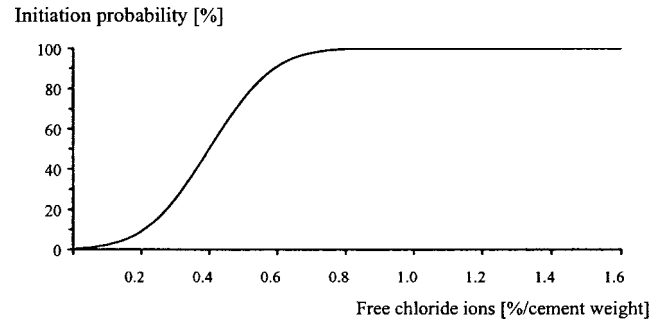**Fig. 2.** Development of corrosion of steel reinforcement in concrete with time

Fig. 3. Corrosion initiation probability as function of free chloride ion concentration

cal resistance of the concrete, the permeability of concrete cover (diffusion of hydroxide ions), humidity, and temperature.

Model Description

The developed model for corrosion-induced deterioration of reinforced concrete consists of the following elements:
- A numerical model of chloride penetration;
- Triggering conditions for corrosion initiation, defined as a function of chloride content at reinforcement level; and
- A simplified model of corrosion propagation (section loss) based on available experimental data.

A relation between the estimated extent of corrosion and a visual appearance of the concrete surface is established to convert the results of the deterioration model to condition states.

Chloride Penetration

Water Transport. Water is the principal means of the transport for chlorides in concrete, carrying dissolved chlorides from the concrete surface to the interior. The two main mechanisms responsible for the water transport in concrete are capillary action (liquid phase) and diffusion (mainly for vapor phase).

Although complex water transport models have been developed (Oberbeck 1995; Flückiger et al. 1996; Janz 1997; Johanesson 1998), a simple unidirectional model is used in this study. It enables the simulation of real in situ exposure taking into account variations of the ambient relative humidity.

In the model developed, both water transport mechanisms (capillary action and diffusion) are modeled with the diffusion equations. With capillary suction the suction depth is governed by the equilibrium between the water surface tension and the weight of capillary water. Although this phenomenon is significantly different from diffusion, the same analytical model for diffusion can be applied and the effect of capillary suction can be numerically approximated using a diffusion model. For this purpose, according to experimental results, it is necessary to vary diffusion coefficient with respect to the concrete depth (Fig. 3).

Diffusion is modeled by Fick's first law

$$J_w = -D_w \cdot \nabla w \qquad (2)$$

where J_w, the flux of water, is proportional to the gradient of evaporable water content ∇w. D_w=water diffusion coefficient, defined by (Bazant 1986) as a function of the relative humidity h_r, to take into account the vapor and liquid phase of the water

$$D_w = D_{100\%} \cdot \left(0.05 + \frac{0.95}{1 + 3 \cdot (1 - h_r)^4} \right) \qquad (3)$$

The relative humidity h_r can be obtained for sorption and desorption by using the following equations:

$$w = w_{sat} \cdot h_r \quad \text{desorption} \tag{4}$$

$$w = w_{sat}(1.16 \cdot h_r^3 - 1.05 \cdot h_r^2 - 0.11 \cdot h_r + 1) \quad \text{sorption} \tag{5}$$

The evaporable water content is w and the maximum evaporable water content is w_{sat} (140 kg/m^3 in this study) (Bazant 1986; Saetta et al. 1993).

The transport of the water in the vapor phase is additionally dependent on temperature. The diffusion coefficient D_{wT} at temperature T is given by

$$D_{wT} = D_w \cdot \exp \frac{E}{R}\left(\frac{1}{T_0} - \frac{1}{T}\right) \tag{6}$$

where E=activation energy (minimal energy necessary to pass from one state to the other); R=gas constant; and T_0=temperature at which the diffusion coefficient D_w has been determined according to Eq. (3) (Saetta et al. 1993; Tang 1996).

To solve Eq. (2), an iterative unidirectional numerical model is used. The element is subdivided into a regular mesh and the wetting conditions are applied as boundary conditions at the surface of the element. At each time increment, the water content is determined at each node of the mesh. Subsequently the relative humidity and diffusion coefficients are recalculated at each node [Eqs. (3)–(6)].

Chloride Transport. Chloride ions can exist in concrete in two forms; as free chloride ions, which are dissolved in water, and as chemically bound chlorides that have reacted with the cement paste. The ratio γ, between the free chloride ion content in the pore solution c_f and the bound chloride content in the porous body c_s [Eq. (7)] varies between 0.4 and 1.0 according to Breit (1998)

$$\gamma = \frac{c_f}{c_s} \tag{7}$$

This ratio varies as a function of time and chemical properties of the cement paste. Complex theoretical models including variation with respect to time have been developed by (Johannesson 1998; Lunk et al. 1998). In this study, as experimental data do not exist, the ratio is taken as 0.6. This is a good approximation for long-term calculations according to Lunk et al. (1998) and Breit (1998).

The two methods of chloride transport in water, the "piggybacking" of chlorides by water and the diffusion of chloride ions, are formulated with Fick's second law
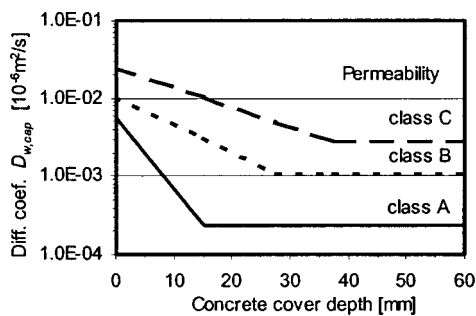

Fig. 4. Variation of average diffusion coefficient for concrete cover permeability classes

Table 2. Condition State Criteria Mapped to KUBA-MS Definitions

Transition	Condition state
CS 1	<0.2% free Cl$^-$/mass of cement
CS 2	<50 μm of reinforcement radius loss
CS 3	<10% of reinforcement section loss
CS 4	<25% of reinforcement section loss
CS 5	>25% of reinforcement section loss

$$J_{Cl} = -D \cdot \nabla C_f \tag{8}$$

where J_{Cl}=flux of chloride ions; and C_f=content of free chloride ions (kg/m^3) of concrete. The theorem of mass conservation can be expressed by Fick's first law

$$C_t = -\text{div} \, J_{Cl} \tag{9}$$

where C_t=total content of chloride; the sum of the free and bound chloride ions, C_f and C_s, respectively,

$$C_t = C_f + C_s \tag{10}$$

Using the relation between the total chloride mass and the concentration of the free and bound chloride ions, Eq. (10) becomes

$$C_t = w \cdot c_f + (1 - w_{sat}) \cdot c_s \tag{11}$$

where c_f=concentration of free chloride in water; c_s=ratio of bound chloride content and water content; and w=water content (L/m^3). By introducing Eq. (11) into Eq. (8), the flux of chloride ions is given by

$$J_{Cl} = -D_{Cl} \cdot w \frac{dc_f}{dx} - D_w \cdot c_f \frac{dw}{dx} \tag{12}$$

where D_{Cl}=chloride diffusion coefficient in the water; and D_w=water diffusion coefficient.

The first part of this equation, representing the chloride diffusion, is solved with the same iterative numerical model that is used to solve the water diffusion transport. The second part of the equation, representing the piggybacked chlorides, is solved as follows:

1. In the numerical model, the water flow is solved first according to Eq. (2) yielding the water gradient. The speed of the water V_w can be therefore calculated at each node of the mesh as

$$V_w = D_w \cdot \frac{dw}{dx} \tag{13}$$

2. The speed of the chlorides V_{Cl} is lower than the speed of the water due the filter effect of the cement paste (Lunk et al. 1998). The speed is obtained by multiplying the water speed with a retardation coefficient R_{Cl}.

$$V_{Cl} = (1 - R_{Cl}) \cdot V_w \tag{14}$$

Table 3. Concrete Cover Air Permeability Measured with Commercial Device (Torrent and Frenzer 1995) for Three Concrete Cover Permeability Classes

Concrete cover permeability class	Torrent permeability coefficient kT (10^{-16} m^2/s)
A	$kT < 0.2$
B	$0.2 < kT < 2.0$
C	$kT > 2.0$

Table 4. Average Diffusion Coefficients for Concrete Cover Permeability Classes

Concrete cover permeability class	Torrent permeability coefficient kT $(10^{-16}\,\mathrm{m^2/s})$	Water diffusion coefficient		Chloride diffusion coefficient D_{Cl} $(10^{-12}\,\mathrm{m^2/s})$
		Diffusion D_w $(10^{-12}\,\mathrm{m^2/s})$	Capillary suction $D_{w,cap}$ $(10^{-12}\,\mathrm{m^2/s})$	
A	0.1	60	vary in function	6
B	1	130	of the depth	13
C	10	200	(Fig. 4)	20

3. At each node of the mesh, the chloride content is finally calculated using speed of the chloride ions.

Corrosion Initiation

The corrosion initiation time is the time it takes chloride ions to reach a certain critical concentration at the reinforcement level. A summary of recent research showed that a wide range for the critical chloride ion concentration has been measured. A ratio of 0.4% of total chloride ions to cement weight is frequently used. This value, however, is often overly pessimistic with regard to the initiation time of corrosion for in situ conditions (Breit 1998).

The probability of corrosion initiation in this study is taken as a function of the free chloride ion concentration as shown in Fig. 4. A normal distribution is assumed with an average value of 0.4% and a standard deviation of 0.15%.

Corrosion Propagation. The chloride-induced corrosion is an electrochemical process. At the reinforcement level, an anode and a cathode are created. At the anode, when the protective passive layer becomes instable due to the presence of Cl^- ions, the iron oxidizes, dissolves, and reacts with the hydroxide resulting in the formation of various rust products. At the cathode, the electrons produced at the anode are consumed by the formation of hydroxide ions. The rate of the reaction is governed by the supply of the reacting products. Generally, with the exposure to outdoor environmental conditions, the supply of hydroxide ions at the anode governs the rate of corrosion.

From the measurement of the corrosion current, it is possible to establish the reacted mass of the reinforcement by the Faraday equation

$$m_{corr} = \frac{i \cdot t \cdot a}{n \cdot F} \tag{15}$$

Table 5. Exposure Zones of Segments to Chloride Contaminated Water

Exposure zones	Segments
Direct (direct contact with water)	Curb (inner side)
	Deck (top side):
	Infiltration (leak)
	Water evacuation system
Splash (splashed by passing vehicles)	Curb (exterior side)
	Deck (underside): Flow
	Pile and strut
	Retaining wall
Mist (contact with mist generated by passing vehicles)	Deck (underside)
	Pile and strut
	Abutment and walls
	Other parts

where m_{corr}=reacted mass; i=current density; a=atomic mass; t=time; F=Faraday constant; and n=number of equivalent changes. The experimental and model results available in the literature show the relative influence on the corrosion current of the electrical resistance of the concrete, the permeability of concrete cover (diffusion of hydroxide ions), humidity, exposure, and temperature. The active corrosion of the reinforcement is typically modeled by the reduction of the diameter of the reinforcement bars with respect to time.

The chloride corrosion considered is the uniform distributed corrosion that leads to the surface damage of the concrete (spalling). However, with the chloride-induced corrosion, pitting also occurs and has faster corrosion rates. As the pitting corrosion does not create significant surface damage and does not induce significant intervention costs, this phenomenon is not considered in the BMS.

Integration into Bridge Management Systems

As in BMSs only discrete condition states are used, the continuous variables in deterioration models must be discretized (condition state, exposure to chloride ions, and corrosion rates).

Condition State

For existing condition states, which are defined by their visual appearance, corresponding quantitative physical and chemical criteria are established (Table 2). In other words the visual appearance is mapped to a set of quantitative criteria.

A segment in the condition State 1 is defined as having a free chloride ion content of less than 0.2% of cement mass. This value is chosen because at this percentage, the estimated corrosion initiation probability is less than 10% and no deterioration is expected.

Condition States 2, 3, 4, and 5 are all defined in terms of reinforcement section loss. Condition State 2 is defined as the section loss that leads to the propagation of the corrosion cracks into the concrete cover. Researchers, notably (Hansen and Saouma (1999), show that this value varies according to parameters such as the concrete tension resistance, elastic modulus, and cover depth. However, as even a little section loss leads to crack propagation, the time necessary for cracks to reach the surface is estimated as only a few years once corrosion has started. In this study it is assumed that section loss alone governs the appearance of cracks on the concrete surface.

A segment is classified as condition State 3 when the reinforcement loss is estimated between 50 μm of the radius and 10% of total cross section. A section loss of 10% is selected for the upper limit of condition State 3 and the beginning of condition State 4 because the change in structural behavior is negligible with less than 10% section loss, although the concrete shows local damages.
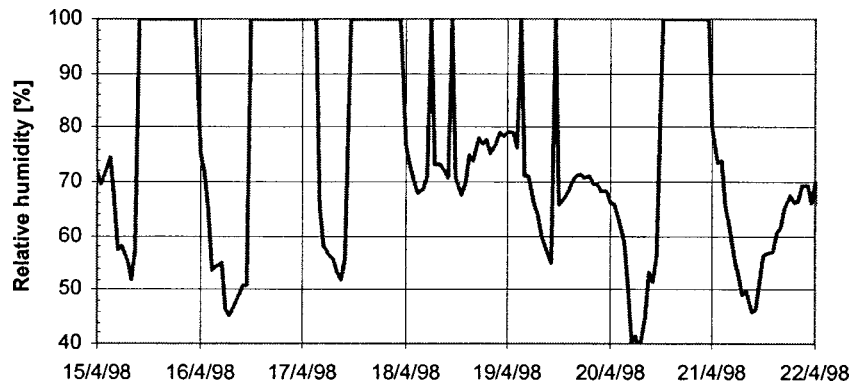
Fig. 5. Sample of relative humidity of environment used in simulations

A segment in condition State 5 is defined as having a section loss of greater than 25%. Condition State 5 is a state of alarm where safety is assumed to be jeopardized. As previously mentioned, there is no inherent correlation between the condition state and the structural role of the element. Analysis of existing structures showed that a section loss of 25% in the crucial load carrying elements changed the structural behavior and reduced the safety margin significantly.

Concrete Cover Properties

Three concrete cover permeability classes are defined based on a nondestructive quantitative measurement of the concrete permeability (Table 3).

The water and chloride diffusion coefficients assumed for each concrete cover permeability class are presented in Table 4 according to the relations between the permeability coefficient kT and the diffusion coefficients. These values are based on

1. The water diffusion coefficients (representing capillary suction) $D_{w,cap}$, adjusted to fit capillary suction tests found in literature;
2. The water diffusion coefficient (real diffusion), D_w, from tests found in literature for concretes of equivalent concrete permeability (Dhir and Byars 1993; Halamickova and Detwiler 1995; Delagrave et al. 1996); and
3. The chloride diffusion coefficient, D_{Cl}, from chloride penetration tests in saturated concrete, notably Lunk et al. (1998) and Torrent and Frenzer (1995) and measures of concrete cover permeability.

In situ measurements on the investigated bridges (Adey et al. 1998) showed a great spatial variation of the values. To take this into account, simulations of chloride penetration are performed for each concrete cover permeability class for various diffusion coefficients selected to represent a normal distribution with a variance of 25%.

Exposure to Chloride Contaminated Water

Three exposure zones are defined (Table 5). The humidity conditions used in the simulations are derived from meteorological records (Fig. 5). The liquid water in contact with the concrete surface, leading to capillary suction as transport mechanism, is assumed for each exposure zone as given in Table 6.

Exposure to Chloride Ions

The chloride concentration of water is assumed to be a constant 2% yielding a saline solution with a freezing point of -1.8%. As the chloride ion concentration in the water is dependent on the amount of de-icing salt spread on the pavement, this value is determined using the annual total amount of salt spread per road maintenance center and the local meteorological data. No direct measurements of the chloride ion content, the number of salt-truck passes, nor the number of days in which salt was spread are available.

Corrosion Rates

Three corrosion rates are defined, based on measurements (Gonzalez et al. 1995). The rates for each concrete exposure zone and concrete cover permeability class are given in Table 7.

Table 6. Boundary Humidity Conditions for Simulations with Model

Exposure zone	During rainfall	Dry weather
Direct	Day: Contact with water during the rain Night: Contact with water during the rain and then until the morning	Relative air humidity
Splash	Relative humidity during the first hour of rain and then water contact until the end of the rain	Relative air humidity
Mist	Relative humidity	Relative air humidity

Table 7. Corrosion Speed (mm/year) as Function of Concrete Cover Permeability Class and Exposure Zone

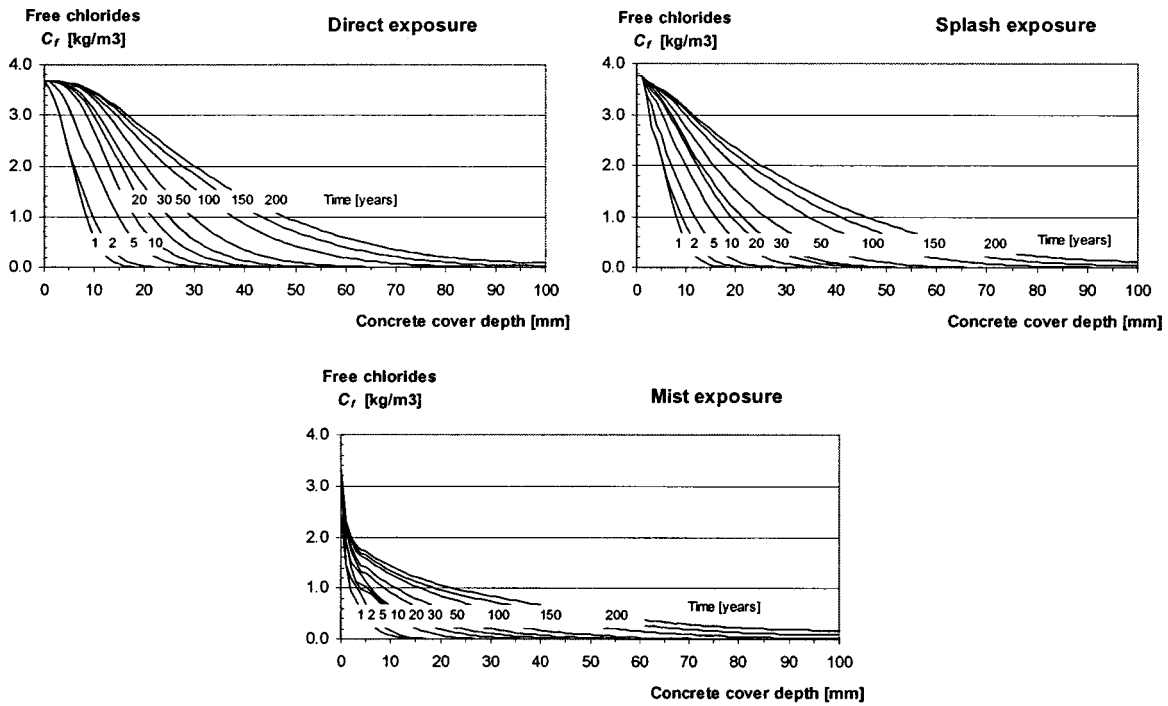| Concrete cover permeability class	Exposure zone		
	Mist	Splash	Direct
A	0.004	0.02	0.02
B	0.004	0.02	0.02
C	0.02	0.08	0.08

Fig. 6. Free chloride ion content profiles calculated with concrete cover permeability Class A and three exposure zones

Deterioration Rates

To classify the condition evolution, three deterioration rates are defined, according to the following definitions:
- Slow: less than 50% in condition States 1 and 2 after 120 years;
- Medium: less than 50% in condition States 1 and 2 after 80 years; and
- Fast: less than 50% in condition States 1 and 2 after 40 years.

Simulations

Condition Evolution

The condition evolution is estimated in three steps:

1. Chloride penetration is simulated for each concrete cover permeability class and exposure zone. In order to take into account the scatter of the permeability, the chloride penetra-
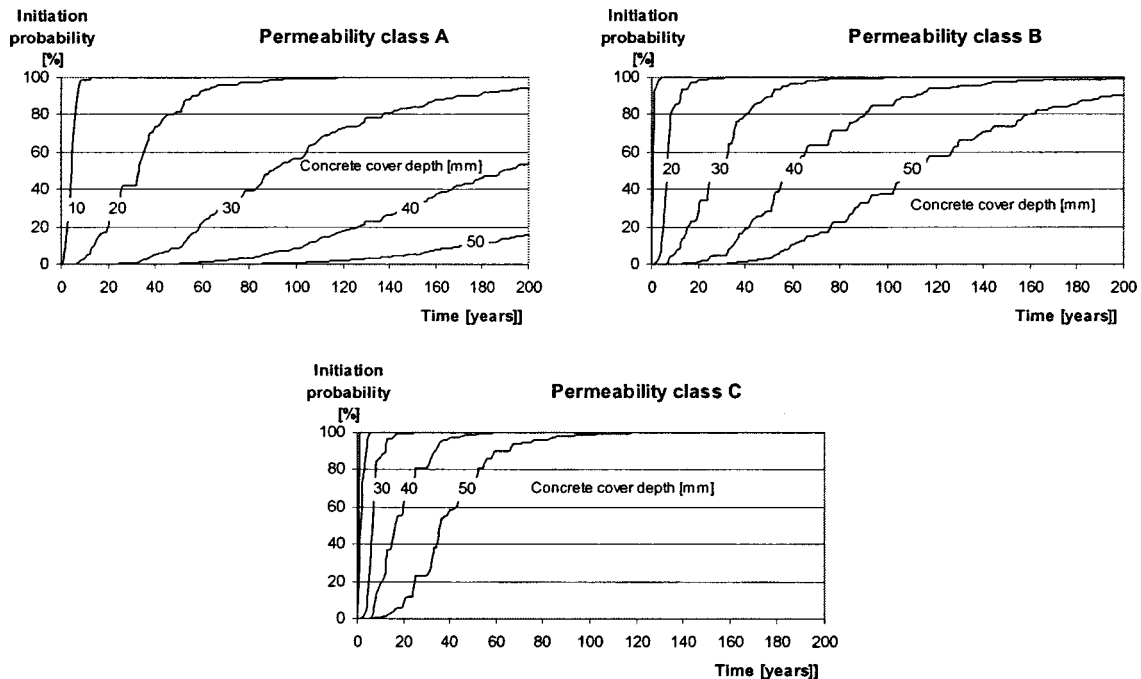

Fig. 7. Probability of corrosion initiation with splash exposure and three permeability classes
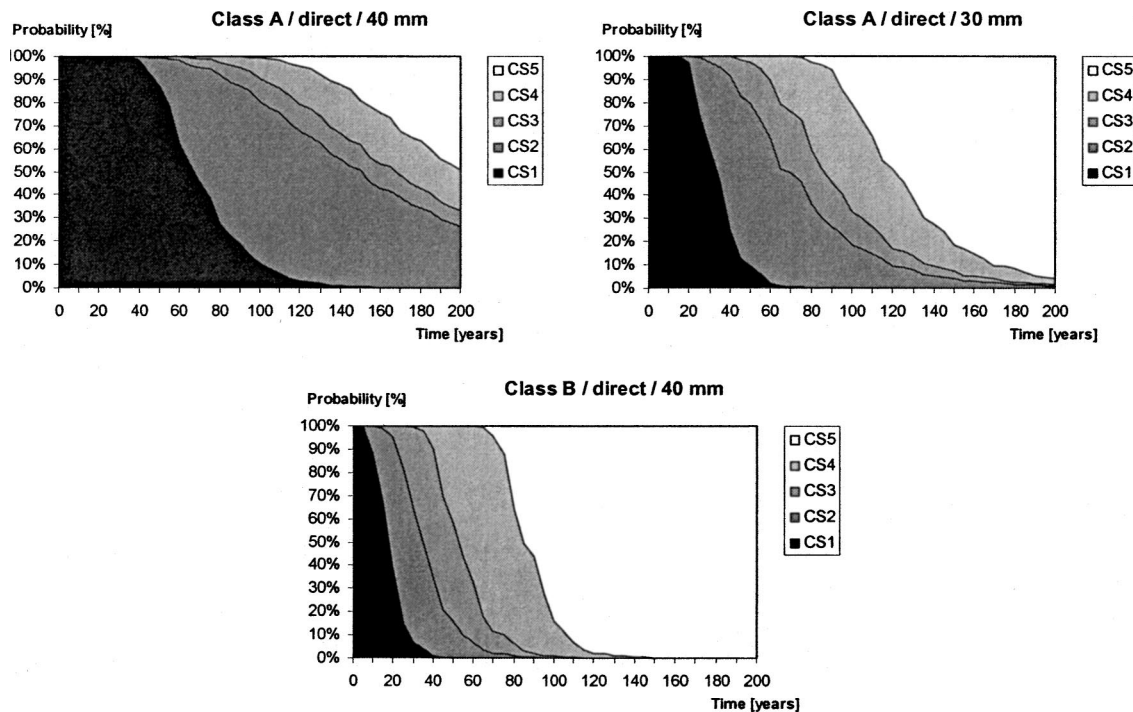
Fig. 8. Condition evolution with splash exposure with various concrete cover depth and concrete cover permeability

tion is simulated for each concrete cover permeability class and exposure zone using a sample of diffusion coefficients selected to match the normal distribution with the mean values given in Table 4 and the variance of 25%. The depths of chloride front and how they vary with time are presented in Fig. 6 for the three exposure zones and the mean diffusion coefficient of permeability Class A.

2. The probabilities of corrosion initiation are determined as a function of time using the assumed initiation condition (Fig. 3) and the distribution of the chloride penetration depths (Fig. 6). The probabilities of corrosion initiation for five different cover depths are presented in Fig. 7 for the three concrete cover permeability classes. A comparison of the results for each permeability class shows that for Class C, the corrosion initiation time is very short even for thick concrete covers.

3. The condition evolution in the propagation phase is estimated deterministically for a given initiation time. In other words there is no increase in uncertainty in the propagation phase (Fig. 8).

The results of all of these simulations can be used to set quality requirements for bridge elements. The required depth of concrete cover corresponding to the three deterioration rates is presented in Table 8 for each concrete cover permeability class and exposure zone. Using this table, it is possible to determine the deterioration rate for a segment from which the condition evolution can be determined, based on visual inspection (to assess exposure) and nondestructive testing (to estimate concrete cover permeability and cover thickness). For instance, if concrete cover permeability of Class A is measured with a thickness of 25 mm and the exposure is observed to be a splash zone, the deterioration rate of the considered segment is medium.

Markov Chains

The condition evolution in KUBA-MS is formulated using Markov chains [Eq. (1)]. The transition probabilities in the deterioration matrices are calculated to yield an optimum fit of the condition evolution predicted using the Markov chains with the condition evolution obtained by using the simulations. The least-square method has been used to determine the optimum fit for condition vectors at 100, 150, and 200 years. The matrices obtained for the three deterioration rates are presented in Table 9.

The difference between the deterioration curves obtained by Markov chains differs significantly from the simulation results. The Markov chains do not consider the initiation time and therefore the curve between condition States 1 and 2 is a power curve, a_{11}^n, where n is the number of intervals. This curve is significantly different from the curve obtained using the deterioration model (Fig. 9). This difference is propagated onto the curves between the other condition states.

Table 8. Concrete Cover Thickness as Function of Concrete Cover Permeability Classes, Exposure Zone, and Deterioration Rate

Concrete cover permeability class	Exposure zone	Deterioration rate		
		Slow (mm)	Medium (mm)	Fast (mm)
	Mist	25	20	15
A	Splash	35	25	20
	Direct	40	30	20–25
	Mist	45	25	15
B	Splash	60	40	30
	Direct	—	50	40
	Mist	—	50	30
C	Splash	—	—	50
	Direct	—	—	—

JOURNAL OF BRIDGE ENGINEERING © ASCE / MAY/JUNE 2004 / **275**

Table 9. Deterioration Markov Chain Matrices

Slow deterioration rate					Medium deterioration rate					Fast deterioration rate				
0.94	0.06	0	0	0	0.87	0.13	0	0	0	0.76	0.24	0	0	0
0	0.97	0.03	0	0	0	0.90	0.10	0	0	0	0.74	0.26	0	0
0	0	0.84	0.16	0	0	0	0.81	0.19	0	0	0	0.75	0.25	0
0	0	0	0.95	0.05	0	0	0	0.91	0.09	0	0	0	0.93	0.07
0	0	0	0	1.00	0	0	0	0	1.00	0	0	0	0	1.00

Conclusions and Outlook

The work presented in this paper leads to the following conclusions:

1. The condition evolution of reinforced concrete elements due to chloride-induced corrosion of the reinforcement can be determined using the theoretical model based on the physical phenomena causing deterioration, visual inspection (for exposure), and nondestructive testing (for concrete cover quality and cover thickness). Numerical data on chloride contamination and the extent of corrosion can be obtained as well.

2. The results can be expressed in the format used in BMS, which is based on visual inspection, by
   • Mapping simulation results to condition states;
   • Establishing permeability classes using permeability measurements; and
   • Classifying the environmental influence.

In such a manner the results from the theoretical model are transformed into BMS format and can be compared quantitatively with those obtained form the classical condition evolution model based on Markov chains. This is particularly useful when there are no or very few inspection data on heavily deteriorated elements.
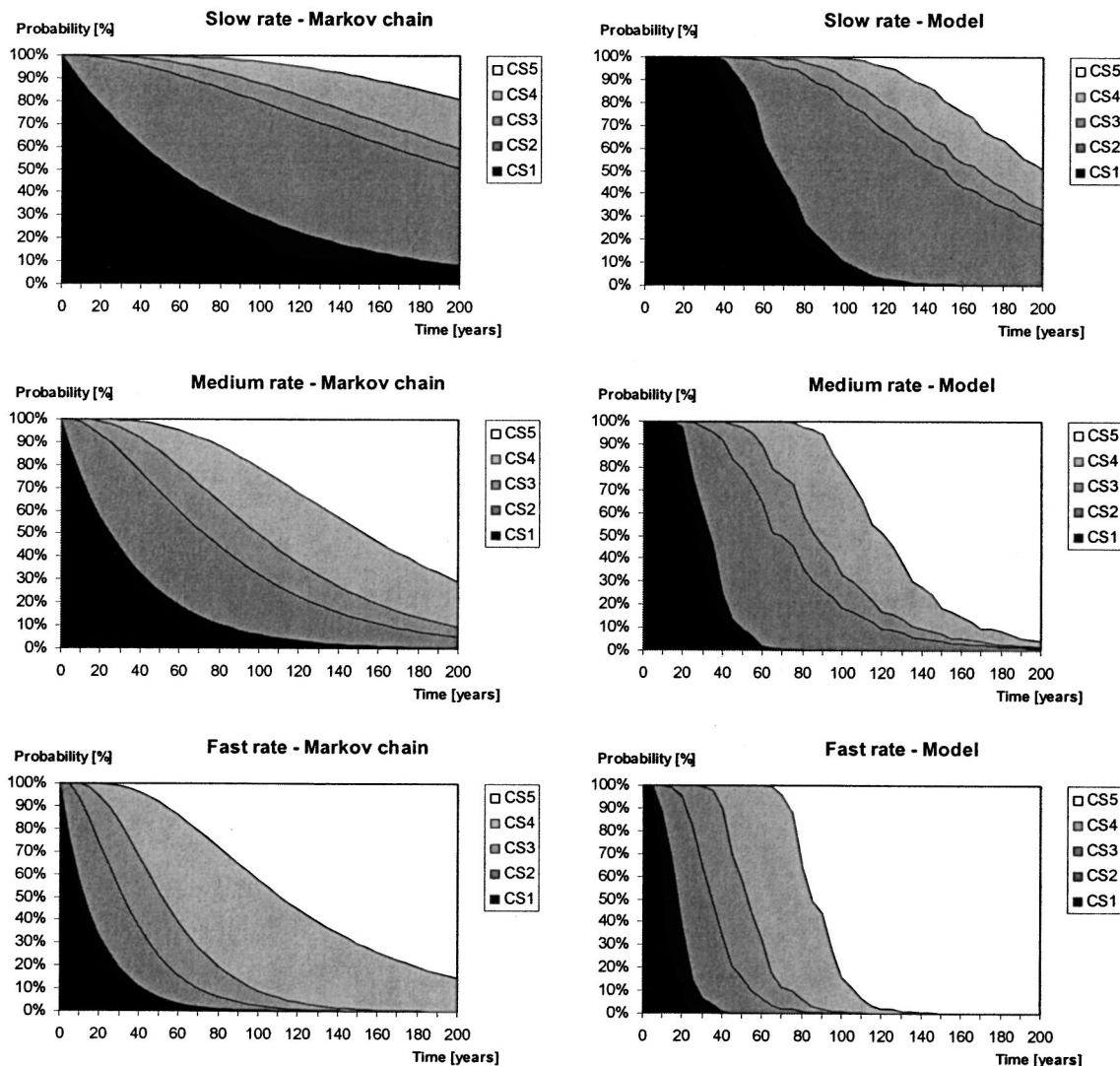

Fig. 9. Deterioration curves obtained with fitted Markov chains and curves obtained with theoretical deterioration model

3. The deterioration curves obtained with Markov chains do not have the same shape as the ones obtained by modeling the deterioration phenomena. This is mainly because the initiation time cannot be modeled by the traditional Markov chain formulation. It is therefore necessary to refine the Markov chain models, e.g., introduction of hidden states, to address mentioned deficiencies in the future.

4. It is shown that the results obtained using the model presented in this paper can be readily mapped to condition states. The modeling parameter (depth of concrete cover and concrete permeability) can be easily updated by inspection. This raises the question of whether models, such as the one presented in this paper, should be directly used in BMSs instead of Markov chains. The strength of Markov chains, however, is with the optimization of possible preservation actions, which is not discussed in this paper. By using Markov chains to model deterioration the optimum set of preservation actions for the element can be formulated as a Markov decision process, which can be easily solved using linear programming techniques. The same optimization problem using deterioration functions obtained by means of the model described in this paper would most likely be much harder to solve. For this reason it seems feasible at least in the foreseeable future to continue to use Markov chain models in BMSs.

Notation

The following symbols are used in this paper:

a = atomic mass;
$a_{i,j}$ = deterioration matrix coefficient;
C_f = free chloride ion content (in concrete);
C_s = bound chloride ion content (in concrete);
C_t = total chloride ion content (in concrete);
CS_i = condition state;
c_f = free chloride ion content solved;
c_s = bound chloride content (in porous body);
D_w = water diffusion coefficient;
$D_{w,cap}$ = water diffusion coefficient with capillary suction;
D_{wT} = water diffusion coefficient in function of temperature;
$D_{100\%}$ = water diffusion coefficient with saturated concrete;
E = activation energy;
F = Faraday constant;
h_r = relative humidity;
i = density current;
J_{Cl} = chloride ion flux;
J_w = water flux;
kT = Torrent permeability coefficient;
m_{corr} = reacted mass of the reinforcement;
n = number of equivalent changes;
R = gas constant;
R_{Cl} = retardation coefficient;
T = temperature;
T_0 = temperature at which D_w has been determined;
t = time;
V_{Cl} = chloride ion speed;

V_w = water speed;
w = evaporable water content;
w_{sat} = maximum evaporable water content;
x_i = condition state coefficient of condition state vector; and
γ = ratio between bound and free chloride ion.

References

Adey, B., Roelfstra, G., Hajdin, R., and Brühwiler, E. (1998). ''Permeability of existing concrete bridges.'' *Proc., 2nd Int. PhD Symp. in Civil Engineering*, Budapest, Hungary, 110–117.

Bazant, Z. P. (1986). ''Creep and shrinkage of concrete: mathematical modelling.'' *Proc., 4th RILEM Int. Symp.*, Ill.

Breit, W. (1998). ''Critical corrosion inducing chloride content—State of the art (Part I).'' Betontechnische Berichte, 442–449.

Delagrave, A., Marchand, J., and Samson, E. (1996). ''Prediction of diffusion coefficients in cement-based materials on the basis of migration experiments.'' *Cem. Concr. Res.,* 26(12), 1831–1842.

Dhir, R. K., and Byars, E. A. (1993). ''PFA concrete: Chloride diffusion rates.'' *Mag. Concrete Res.,* 45(162), 1–9.

Flückiger, D., Elsener, B., and Böhni, H. (1996). ''Chloride in concrete—transport and assessment, chloride im Beton: Transport und Erfassung.'' *Rep. No. 520*, Union des Professionnels Suisses de la Route (VSS), Zürich, Switzerland.

Gonzalez, J. A., Andrade, C., Alonso, C., and Feliu, S. (1995). ''Comparison of rates of general corrosion and maximum pitting penetration on concrete embedded steel reinforcement.'' *Chem. Concr. Res.,* 25(2), 257–264.

Halamickova, P., Detwiler, R. J., Bentz, D. P., and Garboczi, E. J. (1995). ''Water permeability and chloride ion diffusion in portland cement mortars: Relationship to sand content and critical pore diameter.'' *Chem. Concr. Res.,* 25(4), 790–802.

Hansen, E., and Saouma, V. E. (1999). ''Numerical simulation of reincorced concrete deterioration—Part II: Steel and concrete cracking.'' *ACI Mater. J.,* 96(3), 331–338.

Janz, M. (1997). ''Methods of measuring the moisture diffusivity at high moisture levels.'' *Rep. No. TVBM-3076*, Univ. of Lund, Lund, Sweden.

Johannesson, B. (1998). ''Modeling of transport processes involved in service life prediction of concrete—Important principles.'' *Rep. No. TVBM-3083*, Univ. of Lund, Lund, Sweden.

KUBA-MS-Ticino—User's manual, Release 1.0. (1998). Federal Department of Highways, Bern, Switzerland.

Lunk, P., Mayer, G., and Wittmann, F. H. (1998). ''Influence of the chloride ingress on the service life of reinforced concrete structures.'' *Rep. No. 536*, Union des Professionnels Suisses de la Route (VSS), Zürich, Switzerland.

Oberbeck, N. (1995). ''Non-stationary heat-humidity- in concrete—Theory and calculations.'' *Rep. No. 95-79*, TU Braunschweig, Germany (in German).

Saetta, A. V., Scotta, R. V., and Vitaliani, R. V. (1993). ''Analysis of chloride diffusion into partially saturated concrete.'' *ACI Mater. J.,* 90(5), 441–451.

Tang, L. (1996). ''Concrete transport in concrete—measurement and prediction.'' *P-96:6 Abstract No. 546*, Chalmers Univ., Chalmers, Sweden.

Torrent, R., and Frenzer, G. (1995). ''Measurement methods and assessment of in situ the concrete cover properties.'' *Rep. No. 516*, Union des Professionnels Suisses de la Route (VSS), Zürich, Switzerland (in German).